Colloids and Surfaces A 568 (2019) 277–283

Contents lists available at ScienceDirect

Colloids and Surfaces A

journal homepage: www.elsevier.com/locate/colsurfa

Cellulose microfibril networks in hydrolysed soy protein isolate solutions

Roland Gouzy[a,b,*], Christos Tsekou[a], Caroline Remijn[a], Krassimir P. Velikov[a,b,c,*]

[a] Unilever R&D Vlaardingen, Olivier van Noortlaan 120, 3133 AT Vlaardingen, the Netherlands
[b] Institute of Physics, University of Amsterdam, Science Park 904, 1098 XH Amsterdam, the Netherlands
[c] Soft Condensed Matter, Debye Institute for Nanomaterials Science, Utrecht University, Princetonplein 1, 3584 CC Utrecht, the Netherlands

GRAPHICAL ABSTRACT

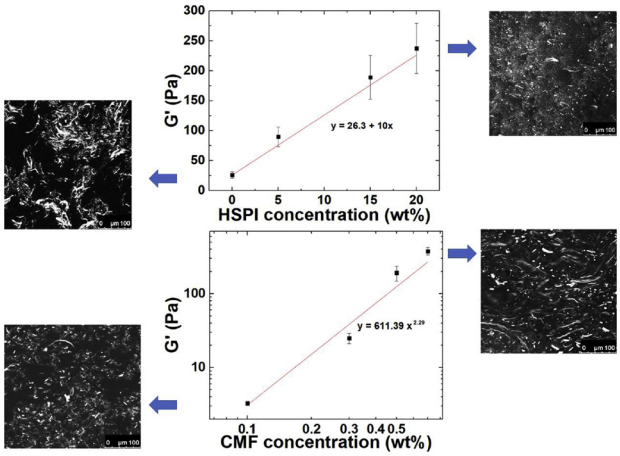

ARTICLE INFO

Keywords:
Cellulose microfibrils
Hydrolysed soy protein isolate
Rheology
Homogeneity
Hybrid networks

ABSTRACT

Cellulose microfibrils (CMFs) are an intensely studied soft matter system for applications in food and beverage products. CMF dispersions can contribute to products texture and stability through their ability to influence rheology and to reinforce structure of composites. Here we study CMFs dispersions from bacterial origin in the presence of hydrolyzed soy protein isolate (HSPI). Applying high energy density mechanical deagglomeration on CMF in the presence of dissolved HSPI leads to large differences in the microstructure of their aqueous dispersions. The CMF networks are becoming more homogenous as quantified by confocal scanning laser microscopy. By increasing the concentration of CMF, at constant HSPI concentration, we observed a transition from a liquid like to a soft solid like behavior. The elastic properties in all cases are dominated by CMFs. CMF-HSPI hybrid material displays highly tunable mechanical properties which can find applications in texture control of food products.

1. Introduction

Stability and mechanical properties of several food systems can be strongly affected by two major structuring agents; proteins and carbohydrates [1]. Plant based proteins have been broadly used in food formulations as a major ingredient due to their functional properties and nutritional value [2,3]. Soy proteins, in particular, are interesting due to their high protein quality (i.e. digestibility and quantity of

* Corresponding authors at: Unilever R&D Vlaardingen, Olivier van Noortlaan 120, 3133 AT Vlaardingen, the Netherlands.
E-mail addresses: roland.gouzy@unilever.com (R. Gouzy), krassimir.velikov@unilever.com (K.P. Velikov).

https://doi.org/10.1016/j.colsurfa.2019.02.034
Received 30 November 2018; Received in revised form 13 February 2019; Accepted 14 February 2019
Available online 14 February 2019
0927-7757/

essential amino acids) which is combined with good functional properties such as foaming, emulsification, and gelation [4]. Hydrolyzed soy protein isolate (HSPI) has good dispersibility and solubility and is commonly used as a swelling, gelling, foaming and emulsifying agent [5]. However it brings some negative aspects such as lower viscosity and poorer mechanical strength upon gelation compared to the native soy protein isolate [6]. HSPI can be added in hydrophilic and hydrophobic polymer materials (e.g. plasticizers) to modify their properties [7]. The addition of polysaccharides affects significantly the physical properties of soy proteins through the rheological modification of the dispersions and the interactions with the protein [8–10].

The use of water insoluble carbohydrates, polysaccharides such as cellulose is expanding their role in food. Cellulose microfibrils (CMF), the natural building blocks in plants, are an abundant natural biopolymer found in many food systems [11,12]. CMFs are mainly obtained from plants or produced by some bacteria [11]. By applying high energy density mechanical deagglomeration process (i.e. by using microfluidizer or high-pressure homogenizer) to CMFs dispersions, the microfibrils can be temporarily separated and rearranged. Because of their attractive nature, however, the CMF tent to aggregate again: at sufficiently high concentrations they form gels of three-dimensional fibril network [13,14]. The CMF forms a highly entangled network driven by OH-group-mediated H-bonds and van der Waals interactions.

CMFs have already found promising applications in food systems because of its unique fibrillar structure compared to unprocessed cellulose containing dispersions such as plant tissues [15–17]. Bacterial cellulose (BC) has gained attention because of it enhanced functional properties, like mechanical properties, as it is a thickener and gelling agent in food systems [18,19]. The gel-like properties of CMFs combined with its complete indigestibility made this an attractive natural structurant for food products. Several previous studies described and characterized the texture and rheology of CMFs from BC dispersions [20,21].

Composite systems with CMFs and proteins and their interactions have been previously studied for both food and nonfood applications [22]. Novel biobased composites made from CMFs and soy protein were shown to have remarkable mechanical and physical properties. Porous materials with interesting modified water sorption and mechanical properties have also been created from these composites [23]. Concerning food applications, protein-CMF mixtures have been studied and showed that CMFs play a major role in the texture of these mixtures [24]. In all cases, the structure and rheology of the CMFs dispersions in the presence of the proteins play an important role in the systems when used as precursors for composite materials. Glycinin and β-conglycinin, the two main proteins present in soy, are known to adsorb cellulose surfaces [22]. It is therefore expected, that the presence of soy proteins can strongly affect how CMFs interact and the microstructure of their dispersions.

Here we investigate how the structure and the rheology of CMF dispersions will be affected by the presence of HSPI. By using high-pressure homogenization, CMFs are dispersed in the presence of dissolved HSPI. The microstructure and rheological properties will be examined as a function of the CMF and HSPI concentration.

2. Materials and methods

2.1. Preparation of bacterial cellulose dispersion

Bacterial cellulose (BC) was sourced from Cups of Nata de Coco (Sari Kelapa Murni, PT Menacoco Sari). Nata de Coco cubes were homogenized using a multi-mixer (4185545, Braun, Germany) and washed with demineralized water (Barnstead Nanopure Diamond, resistance 18 MΩ cm). Each washing step consisted of rinsing the dispersion over a vacuum filter (Whatman Schleicher and Schuell 113, wet-strengthened circles, 185 mm in diameter) and re-dispersing the residue in 2.0 L of demineralized water using again a multi-mixer (Braun 4185545). After seven washing steps we assumed that all the water-soluble sugars and other additives (i.e., water-soluble colorants, citric acid and sodium benzoate) have been sufficiently removed. The washed retentate was added to 250 mL of demineralized water and subsequently mixed with a Silverson mixer (L5M-A, Silverson, USA) for 10 min at 3800 rpm with a 1 mm holes screen. The concentration of BC was determined by drying 20 g of dispersion in a vacuum oven initially at 105 °C for 24 h. The dry matter content of BC dispersion was measured in triplicate and was determined to be at 1.23 ± 0.01 wt%.

2.2. Preparation of CMF - hydrolysed soy protein isolate (HSPI) dispersions

CMF-HSPI dispersions were prepared using Supro®XT 219D IP, isolated soy protein, hydrolyzed, (90% protein), kindly provided by Danisco Holland B.V., Netherlands. To examine the effect of CMF concentration on the CMF-HSPI suspensions, we dispersed different amounts of concentrated CMF suspension in demineralized water and the right amount of HSPI dry powder to obtain different concentrations of CMF in each CMF-HSPI suspension: respectively 0.1, 0.3, 0.5 and 0.7 wt% at constant concentration, 10 wt%, of HSPI. Each sample had a total volume of 250 mL and was dispersed with a magnetic stirrer at 500 rpm for 10 min. As a control, a solution of 10 wt% solution of HSPI was used.

To examine the effect of HSPI concentration on the CMF-HSPI suspensions, the same procedure as previously was followed, to obtain 0.3 wt% CMF suspensions at three different concentrations of HSPI, respectively 5, 15 and 20 wt%. As a control a solution, a 0.3 wt% CMF was used.

In all cases, each CMF-HSPI mixture was subsequently mixed with a Silverson mixer for 10 min at 3800 rpm with a 1 mm holes screen. The samples were then passed through a Microfluidizer™ (Microfluidics, USA) with a Z-chamber of 87 μm at 1200 bar (1.2×10^5 kPa) to obtain the final dispersion.

2.3. Rheological properties

Rheological measurements of CMF-HSPI mixtures were performed on a stress-controlled rheometer (MCR 302, Anton Paar, Austria), using a sand blasted plate-plate geometry (plate diameter 5 cm, gap 1 mm). The system was temperature controlled with a water bath at a temperature of 20 °C A plastic spoon was used to put the suspension on the bottom plate of the rheometer to minimize shear on the sample. First frequency sweeps were performed in the range of 6.28–188 rad.s^{-1} at a strain of 0.001. Then followed by flow measurements were performed by first increasing the shear rate from 0.1 to 500 s^{-1} in 120 s and then decreasing from 500 to 0.1 s^{-1} in 120 s. All experiments were performed in triplicate, and the results are given as mean values ± standard deviation.

2.4. Confocal scanning laser microscopy (CSLM)

CSLM was performed on a confocal microscope (TGS-SP5, Leica, Germany). For staining, ~5 μL of 0.5 wt% Direct Yellow and 0.5 wt% Rhodamine B aqueous solutions, were added in 1 mL of dispersion to stain the cellulose and the protein, respectively. A droplet of each dyed sample was put on a glass slide for the measurement. Direct Yellow dye was excited at a wavelength of 458 nm and Rhodamine B at a wavelength of 561 nm. The emission wavelength of Direct Yellow is 476–555 nm and for Rhodamine B is 580–700 nm. High magnification images were taken using an oil immersion objective (40 × and 63 × magnification).

For the image analyses, CLSM images at 40 times magnification were used. The mages were converted to 8 bits and then normalized by using the Enhance Contrast normalization option with 0.4% saturated pixels. From the resulting intensity histogram, we define a homogeneity parameter by first determining the full width at half maximum of the

intensity distribution and then dividing this value by 256 (number of grey values) to yield a number between 0 and 1. Three different CLSM micrographs for each concentration were analysed to determine the homogeneity parameter, and the results are given as mean values ± standard deviation.

2.4.1. Scanning Electron Microscopy (SEM)

A tiny volume of each sample (one droplet) was placed on top of a rivet and plunge-frozen in melting ethane. The sample was cryo-planed using a cryo-ultramicrotome (Leica Ultracut UCT EM FCS), to obtain a freshly prepared cross-section. Cryo-planing was done first by using a glass knife and the last sections were made using a diamond knife (Diatome histo cryo 8 mm) at −120 °C.

The rivet was mounted onto a holder and transferred into a Gatan Alto 2500 preparation chamber. To reveal the microstructures under the planed surface, the temperature of the sample was increased for a short while to −90 °C to remove a thin layer of water by sublimation. This yielded a 3D view on the planed sample. The sample was sputter coated with platinum (120 s) for a better SEM contrast and to prevent charging by the electron beam. The sample was imaged using a Zeiss Auriga field-emission SEM at −125 °C and an accelerating voltage of 3 kV.

3. Results and discussion

3.1. Rheological properties of CMF-HSPI dispersions

Sample preparation and their shear history can affect the rheological properties of CMF-biopolymer mixtures [25]. In the first set of experiments, we gradually increase the concentration of CMF in a 10 wt % solution of HSPI. In this process, we deagglomerate and further disperse the CMF, which were initially part of the BC pellicle, by using high energy density mechanical deagglomeration. The increase of CMF concentration in the HSPI dispersions resulted in a profound effect in the rheological properties. Frequency sweep were performed prior to flow measurements. Frequency sweep measurements showed higher storage modulus (G') (Fig. 1a) and loss modulus (G") (Fig. 1b) when the concentration of CMF was increased. We observe an increase of several decades in the G' in the concentration range from 0.3 wt% to 0.7 wt% (Fig. 1a). We can also notice that by increasing the concentration of CMFs, with or without HSPI, the elastic modulus shows a higher frequency independence with increasing the CMF concentration. This finding is in line with previous studies where CMF mixtures with other polymers were studied and showed similar behaviors [17]. At low concentration of CMFs, the system displays a liquid-like behavior. By increasing CMF concentration, we observed a structure which gradually evolve from displaying a liquid-like to a soft solid-like behavior. The G' dependence on the CMF concentration displayed a power law behavior with an exponent of $n = 2.29$ (Fig. 1c). This value is in the same range found in previous studies on the rheology of CMF networks, which depends on the exact system varying from 2 to 5.2 [26,27]. This range can be explained by differences of heterogeneity of the CMFs networks. Standard theories for entangled polymers have exhibited a value of 2.25 [28].

The viscosity of the CMF-HSPI dispersions was measured as a function of the shear rate (Fig. 1d). The decrease in viscosity at higher shear rates indicated a strong shear thinning behavior for all the mixtures, regardless the CMF and HSPI concentration. The mechanical properties and microstructure of CMF-HSPI suspensions are expected to be affected by the nature of the interaction between the surface of the CMFs and the HSPI. It is likely, to expect that the HSPI interacts with the microfibrils, and therefore induce changes in the microstructure [22].

To study the roles of both components in this hybrid structure, we kept the CMF concentration constant and increased the HSPI concentration. Increasing the concentration of HSPI at a constant concentration of CMF shows that the elastic behavior is mainly caused by the CMFs. Even without any HSPI the elastic modulus remains independent from the frequency (Fig. 2a). The viscosity has also increased when increasing the HSPI concentration, by one decade if we compare the minimum with the maximum concentrations of HSPI, for all shear rates studied (Fig. 2d). This increase however is lower when compared to the effect of CMF concentration where more than two decades increase in viscosity is observed between the minimum and the maximum concentrations of CMF at constant HSPI, which is observed for shear rates below 10 s^{-1} (Fig. 1d).

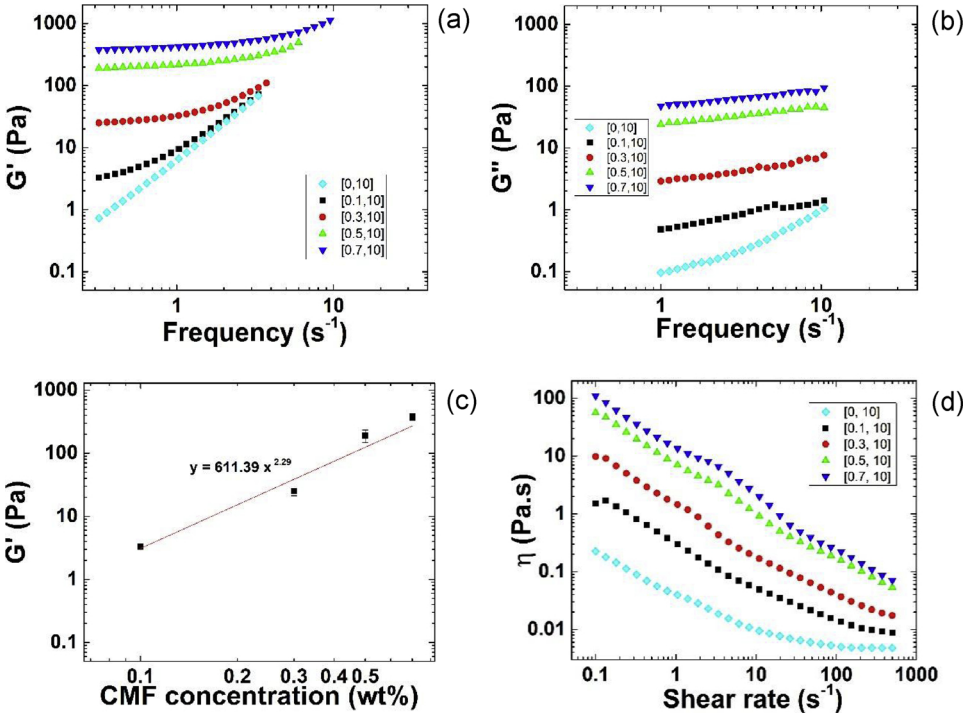

Fig. 1. Rheological properties of CMF-HSPI dispersions of different concentration of CMF in the presence of 10 wt% HSPI. (a) Storage modulus (*G'*) measured at different CMF concentrations as a function of oscillatory shear frequency (ω). (b) Loss modulus (G") as a function of oscillatory shear frequency (ω). (c) Storage modulus (*G'*) at 1 Hz as a function of CMF concentrations. (d) Viscosity (η) as a function of shear rate. Concentrations of CMF (wt%) and HSPI (wt%) are given by [CMF, HSPI].

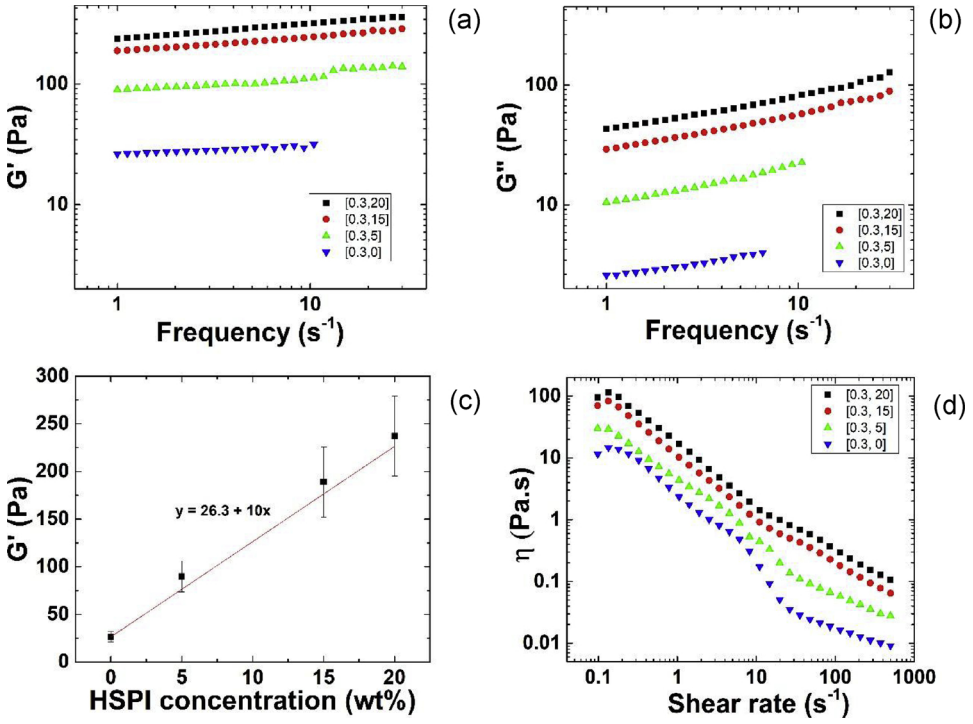

Fig. 2. Rheological properties of CMF-HSPI dispersions with 0.3 wt CMF containing different concentration of HSPI. (a) Storage modulus (*G*') as a function of oscillatory shear frequency (ω). (b) Loss modulus (*G*") as a function of oscillatory shear frequency. (c). Storage modulus (*G*') at 1 Hz of CMF-HSPI dispersions as a function of HSPI concentration. (d) Viscosity (η) as a function of shear rate. Concentrations of CMF (wt%) and HSPI (wt%) are given by [CMF, HSPI].

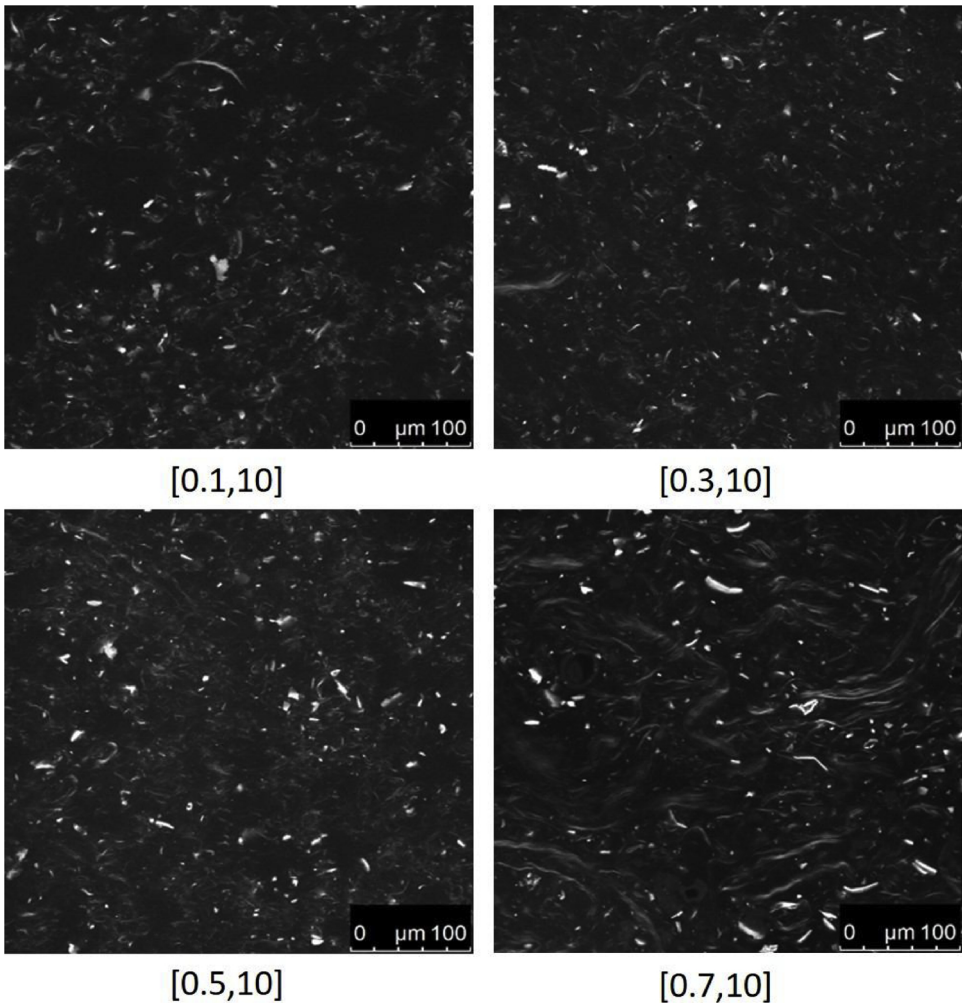

Fig. 3. CSLM images of CMF-HSPI dispersions at constant HSPI concentration. Concentrations of CMF (wt%) and HSPI (wt%) are given by [CMF, HSPI]. Scale bar = 100 μm.

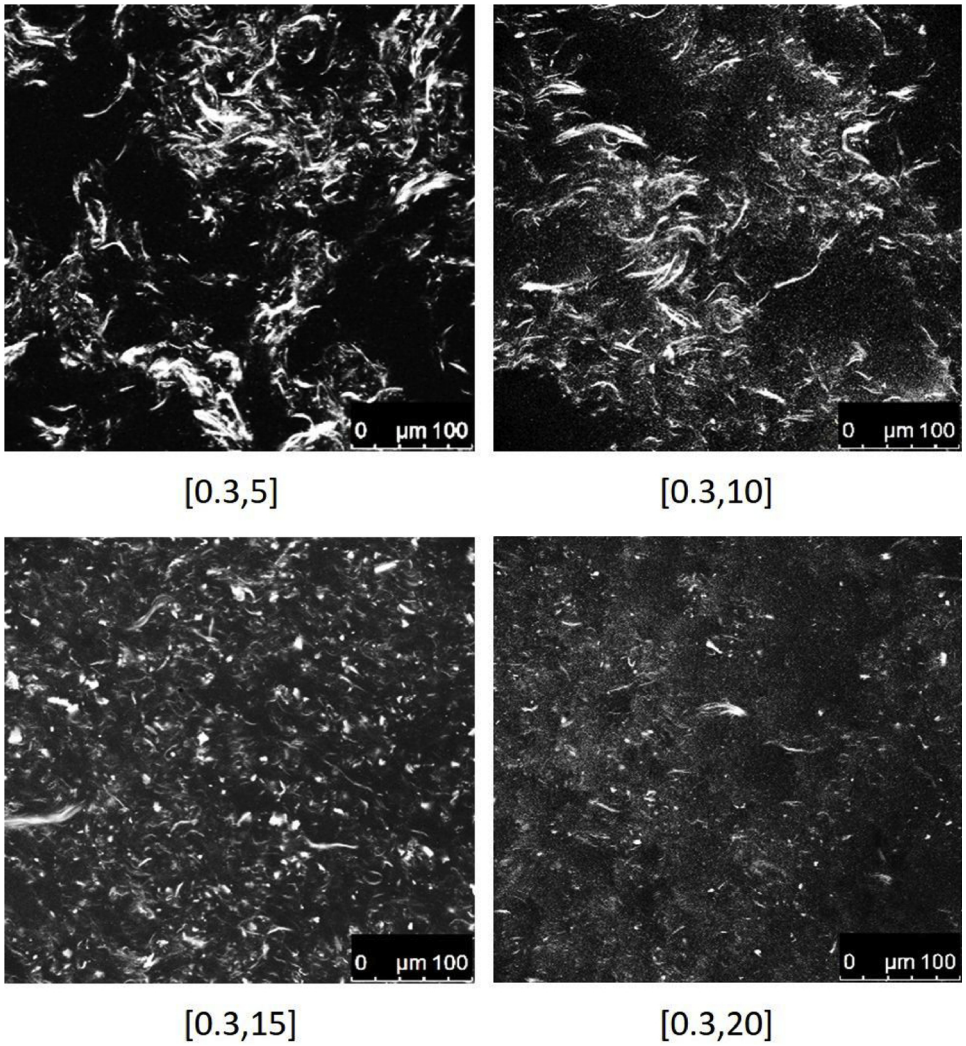

Fig. 4. CSLM images of CMF-HSPI dispersions at different HSPI concentrations at constant CMF concentration. Concentrations of CMF (wt%) and HSPI (wt%) are given by [CMF, HSPI]. Scale bar = 100 µm.

The viscosities of all microfluidized CMF-HSPI suspensions were highly dependent on the concentration of respectively CMF and HSPI (Figs. 1d and 2 d). The suspension with the highest CMF concentration (0.7 wt%) has the highest viscosity compared the highest concentration of HSPI studied (20 wt%), indicating that the network formed by the CMFs is playing a major role in the structuring properties of these dispersions. There is a strong dependence of viscosity at shear rate 10 s^{-1} and lower on concentration with an increase by 3 decades among the different concentrations. The suspensions show shear-thinning across 4 decades of shear rate (Figs. 1d and 2 d). From these data we remark the absence of both high and low shear rate viscosity plateaus.

3.2. Microstructure changes in CMF-HSPI dispersions

To examine the effect of CMF on rheological properties on the CMF-HSPI dispersions, microscopic measurements were performed with a confocal scanning laser microscopy. Dispersing CMF in HSPI solutions resulted in a profound effect in the dispersion microstructure.

The effect of both CMF and HSPI concentration on the microstructure of the formed CMF-HSPI mixed dispersions were examined. By increasing the CMF concentrations at constant HSPI concentration, it is observed that the number of flocs is increasing and subsequently, less voids were observed (Fig. 3). This behavior is similar dispersion of pure CMF from bacterial cellulose [20]. We however observe clear differences with the system of pure CMF: in the presence of HSPI the flocs of CMF are getting dispersed more homogenously. This is already giving some indication of possible interactions between CMFs with the HSPI. At even higher concentration of CMF, we observe even more drastic change: CMFs were still present in the form of flocs, but much longer (> 100 µm) and aligned (most likely under influence of the shear field) (Fig. 4).

By increasing HSPI concentration at constant CMF concentration, the system formed during high-pressure homogenization, became more homogenous as indicate by the increase in the homogeneity parameter (Fig. 5). This is a clear indication that the HSPI, especially at high concentration, i.e. for 0.3 wt% CMF-20 wt% HSPI dispersion, helps to effectively disperse the CMF. As seen with other adsorbing polymers, our results suggest that the attraction between CMFs is weaker with the presence of HSPI which make it easier for the CMF to rearrange in the homogenization process. A plausible origin of this effect is in the adsorption of the proteins on the cellulose surface which the increase zeta potential, hence decrease attraction in between the CMFs [22].

To have a closer look at the microstructure of the CMF-HSPI suspensions, we imaged the suspensions at different concentrations of CMF and HSPI using cryo-SEM, as shown in Fig. 6. High resolution SEM requires a high vacuum, which does not allow wet samples. This was circumvented by quickly freezing the samples in liquid ethane. However, one important artefact is the formation of ice crystals during

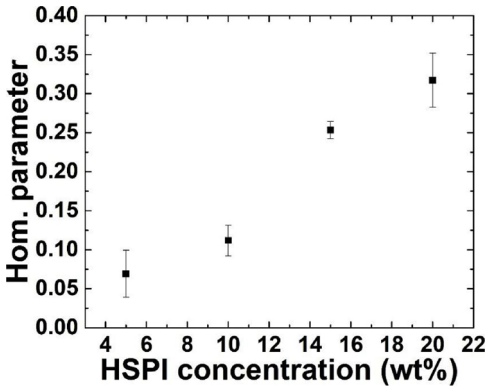

Fig. 5. Homogeneity parameter of the CLSM images (Fig. 4) as a function of HSPI concentration at 0.3 wt% CMF suspensions.

freezing of the material. In general, the freezing artefact is restricted to the sizes of the ice crystals, and therefore, a very quick freezing, resulting in very small ice crystals is preferred. CMFs with the presence of HSPI always appear as bundles where the single fibrils are connected to neighboring fibrils (Figs. 6a and S1). The cry-SEM of pure HSPI (Fig. 6c) reveals the presence of a protein network (see Fig S2). The presence of a protein network is in line with the observed changes in the viscoelastic properties as dependent on the HSPI concentration. When the area where both HSPI and CMF are present was imaged (Fig. 6b and d), we observed less CMFs bundles and flocs. CMF are embedded in the protein network with different degree of deagglomeration (Figs. S3 and S4). The presence of bundled CMF with length larger than several micrometers are still clearly seen. In addition, we also observed the presence of particle-like structures, possibly from the HSPI, at the surface of the CMFs, which is in line with the literature where the protein aggregates even after microfluidization are much large in size [29]. Additional micrographs showing CMF-HSPI mixtures with different concentration are available in the supplementary material (Figs. S1 and S4).

4. Conclusions

We have studied the microstructure and rheological behavior of CMF-HSPI suspensions at different concentrations ratio of both components. The properties of these dispersions are highlighted by an increase of the network homogeneity with the addition of HSPI. CLSM and cryo-SEM imaging have shown significant differences in the microstructure of the CMF networks in presence of the HSPI. The significant increase in homogeneity suggest that the HSPI plays a significant role in moderating the attraction strength between CMFs. The viscoelastic properties of CMF-HPSI suspensions were significantly different from the suspensions with HSPI alone. The presence of CMFs network affects strongly the rheology of these suspensions, the elastic modulus is increased by several decades with the increase of the CMFs concentration. Moreover, the effect of the increase of HSPI concentration is less significant. The results from this study show that CMF dispersion in the presence of HSPI can be obtained with tunable rheology and can be useful for texture design on food products.

Acknowledgements

The authors thank Panayiotis Voudouris for the useful discussions. This research was funded by the European Union within the Horizon 2020 project under the DiStruc Marie Sklodowska Curie Innovative Training Network; Grant Agreement No. 641839 and by NanoNextNL.

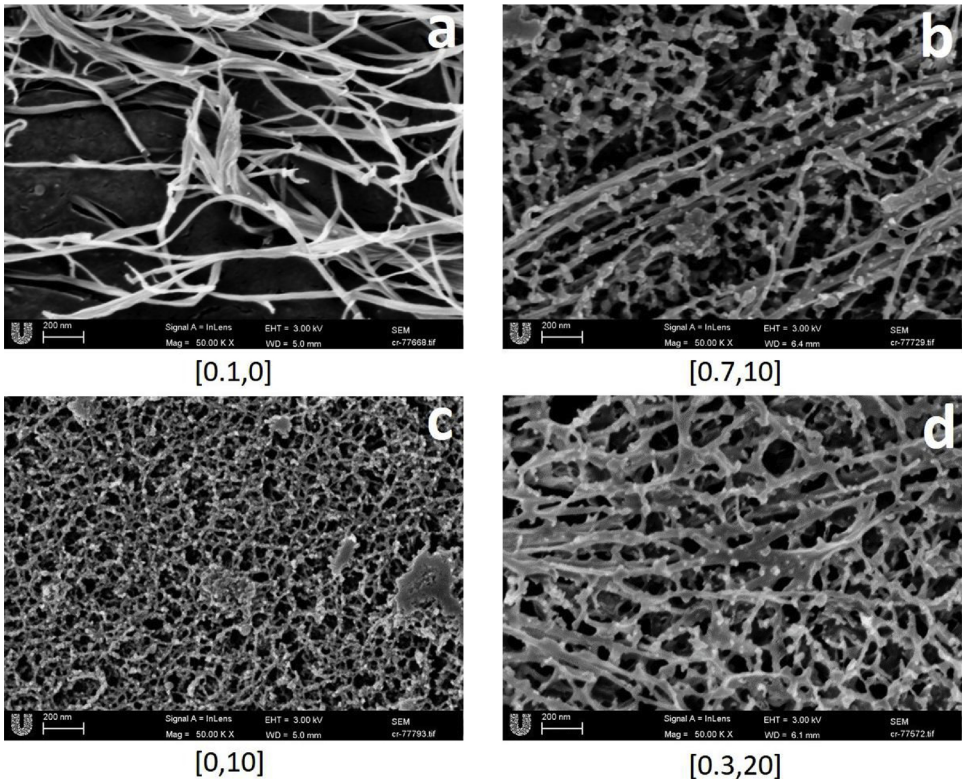

Fig. 6. Representative cryo-SEM images of CMF-HSPI dispersions at different HSPI and CMF concentrations. Concentrations of CMF (wt%) and HSPI (wt%) are given by [CMF, HSPI].

Appendix A. Supplementary data

Supplementary material related to this article can be found, in the online version, at doi:https://doi.org/10.1016/j.colsurfa.2019.02.034.

References

[1] E. Dickinson, Hydrocolloids at interfaces and the influence on the properties of dispersed systems, Food Hydrocoll. 17 (2003) 25–39.
[2] V.R. Young, P.L. Pellett, Plant proteins in relation to human protein and amino acid nutrition, Am. J. Clin. Nutr. 59 (1994) 1203S–1212S.
[3] T.K. Dey, P. Banerjee, R. Chatterjee, P. Dhar, Designing of ω-3 PUFA enriched biocompatible nanoemulsion with sesame protein isolate as a natural surfactant: focus on enhanced shelf-life stability and biocompatibility, Colloids Surf. A Physicochem. Eng. Asp. 538 (2018) 36–44.
[4] J.E. Kinsella, Functional properties of soy proteins, J. Am. Oil Chem. Soc. 56 (1979) 242–258.
[5] A. Achouri, W. Zhang, X. Shiying, Enzymatic hydrolysis of soy protein isolate and effect of succinylation on the functional properties of resulting protein hydrolysates, Food Res. Int. 31 (1998) 617–623.
[6] K. Nishinari, Y. Fang, S. Guo, G. Phillips, Soy proteins: a review on composition, aggregation and emulsification, Food Hydrocoll. 39 (2014) 301–318.
[7] F. Song, D.-L. Tang, X.-L. Wang, Y.-Z. Wang, Biodegradable soy protein isolate-based materials: a review, Biomacromolecules 12 (2011) 3369–3380.
[8] J.-Y. Li, A.-I. Yeh, K.-L. Fan, Gelation characteristics and morphology of corn starch/soy protein concentrate composites during heating, J. Food Eng. 78 (2007) 1240–1247.
[9] Y. Wang, D. Li, L.-J. Wang, B. Adhikari, The effect of addition of flaxseed gum on the emulsion properties of soybean protein isolate (SPI), J. Food Eng. 104 (2011) 56–62.
[10] H. Pan, X. Xu, Y. Tian, A. Jiao, B. Jiang, J. Chen, Z. Jin, Impact of phase separation of soy protein isolate/sodium alginate co-blending mixtures on gelation dynamics and gels properties, Carbohydr. Polym. 125 (2015) 169–179.
[11] I. Siró, D. Plackett, Microfibrillated cellulose and new nanocomposite materials: a review, Cellulose 17 (2010) 459–494.
[12] P. Béguin, J.-P. Aubert, The biological degradation of cellulose, FEMS Microbiol. Rev. 13 (1994) 25–58.
[13] K.J. De France, T. Hoare, E.D. Cranston, Review of hydrogels and aerogels containing nanocellulose, Chem. Mater. 29 (2017) 4609–4631.
[14] S.J. Veen, A. Kuijk, P. Versluis, H. Husken, K.P. Velikov, Phase transitions in cellulose microfibril dispersions by high-energy mechanical deagglomeration, Langmuir 30 (2014) 13362–13368.
[15] F.W. Herrick, R.L. Casebier, J.K. Hamilton, K.R. Sandberg, Microfibrillated Cellulose: Morphology and Accessibility, J. Appl. Polym. Sci.: Appl. Polym. Symp. (United States), ITT Rayonier Inc., Shelton, WA, 1983.
[16] A.F. Turbak, F.W. Snyder, K.R. Sandberg, Microfibrillated Cellulose, a New Cellulose Product: Properties, Uses, and Commercial Potential, J. Appl. Polym. Sci.: Appl. Polym. Symp. (United States), ITT Rayonier Inc., Shelton, WA, 1983.
[17] M.-P. Lowys, J. Desbrieres, M. Rinaudo, Rheological characterization of cellulosic microfibril suspensions. Role of polymeric additives, Food Hydrocoll. 15 (2001) 25–32.
[18] Z. Shi, Y. Zhang, G.O. Phillips, G. Yang, Utilization of bacterial cellulose in food, Food Hydrocoll. 35 (2014) 539–545.
[19] E. Panagopoulou, V. Evageliou, N. Kopsahelis, D. Ladakis, A. Koutinas, I. Mandala, Stability of double emulsions with PGPR, bacterial cellulose and whey protein isolate, Colloids Surf. A Physicochem. Eng. Asp. 522 (2017) 445–452.
[20] A. Kuijk, R. Koppert, P. Versluis, G. van Dalen, C. Remijn, J. Hazekamp, J. Nijsse, K.P. Velikov, Dispersions of attractive semiflexible fiberlike colloidal particles from bacterial cellulose microfibrils, Langmuir 29 (2013) 14356–14360.
[21] D. Lin, R. Li, P. Lopez-Sanchez, Z. Li, Physical properties of bacterial cellulose aqueous suspensions treated by high pressure homogenizer, Food Hydrocoll. 44 (2015) 435–442.
[22] C. Salas, O.J. Rojas, L.A. Lucia, M.A. Hubbe, J. Genzer, Adsorption of Glycinin and β-Conglycinin on silica and cellulose: surface interactions as a function of denaturation, pH, and electrolytes, Biomacromolecules 13 (2012) 387–396.
[23] J.C. Arboleda, M. Hughes, L.A. Lucia, J. Laine, K. Ekman, O.J. Rojas, Soy protein–nanocellulose composite aerogels, Cellulose 20 (2013) 2417–2426.
[24] L. Sun, W. Chen, Y. Liu, J. Li, H. Yu, Soy protein isolate/cellulose nanofiber complex gels as fat substitutes: rheological and textural properties and extent of cream imitation, Cellulose 22 (2015) 2619–2627.
[25] S.J. Veen, P. Versluis, A. Kuijk, K.P. Velikov, Microstructure and rheology of microfibril–polymer networks, Soft Matter 11 (2015) 8907–8912.
[26] S.J. Veen, P. Versluis, A. Kuijk, K.P. Velikov, Microstructure and rheology of microfibril-polymer networks, Soft Matter 11 (2015) 8907–8912.
[27] O. Nechyporchuk, M.N. Belgacem, Fdr. Pignon, Current progress in rheology of cellulose nanofibril suspensions, Biomacromolecules 17 (2016) 2311–2320.
[28] M. Doi, S. Edwards, Dynamics of concentrated polymer systems. Part 3.—the constitutive equation, J. Chem. Soc. Faraday Trans. 2: Mol. Chem. Phys. 74 (1978) 1818–1832.
[29] L. Jong, Characterization of soy protein nanoparticles prepared by high shear microfluidization, J. Dispers. Sci. Technol. 34 (2013) 469–475.